

4 Tension Chord Model for Serviceability Problems

The complex and hardly known *load history* and the *highly variable concrete properties* (see Chapter 3.1) represent the main difficulties for predicting the deformations of reinforced concrete (RC) structural members. For reasons of simplicity, deformation prediction approaches (see Chapter 2) usually neglect the unknown load history (e.g. pre-cracking due to construction overloads) and the corresponding initial deformations. For these reasons, integral (e.g. midspan deflections) and in particular local deformation predictions (e.g. strains, curvatures, crack widths) will never achieve the same accuracy as ultimate load predictions (Marti 1983). Still, practical applications require reasonably reliable estimates of the magnitude of both integral and local deformations.

The Tension Chord Model (see Chapter 3.4) represents a consistent tool for modelling the in-service deformation behaviour of tensile members with uniaxial stress states, such as tension ties and tension chords in one-way bending members. So far (see Chapter 3.4), the model has been used to describe the short-term load- and restraint-induced cracking behaviour of tensile elements (Marti, Sigrist, et al. 1997; 1998; Alvarez 1998) as well as the load-induced cracking and deflection behaviour of statically determinate bending elements (Kenel 2002; Kenel et al. 2005).

Based on this previous work, this chapter aims at illustrating the wide range of serviceability prediction equations for designing tensile and one-way bending members that can be derived based on the Tension Chord Model. Thereto, in Section 4.1 the Tension Chord Model is extended in order to account for the effective concrete area in bending elements, the loss of tension stiffening due to bond creep and the influence of unloading. The Tension Chord Model is then combined with the long-term section deformation approaches for bending elements discussed in Chapter 3.3 to obtain hand-calculation equations for predicting short- and long-term crack widths (Section 4.2) and deflections (Section 4.3). The crack width predictions are focused on moment-, restraint-, and deformation-induced cracking with different boundary conditions. Further, the influence of the reinforcement detailing on the deflections of statically indeterminate members is discussed and limiting span-to-depth ratios are derived. In the whole chapter, the stress in the reinforcement steel is assumed to remain below the yield limit and shear deformations are neglected.

4.1 Tension Stiffening

4.1.1 Short-Term

The Tension Chord Model considers the contribution of the tensile concrete by assuming a linear distribution of concrete tensile stresses between the cracks (Fig. 4.1 (a)). In bending members the concrete stresses are further assumed to be uniformly distributed over the net concrete area $A_{c,ef}$ of a tension chord that has the same centroid as the tensile steel (Fig. 4.1 (c)). This leads to average concrete strains in the tension chord equal to

$$\varepsilon_{c,ts} = \frac{\sigma_{c,ts}}{E_c} = \frac{\lambda f_{ct}}{2E_c} \quad (4.1)$$

Factor λ stands for the crack spacing (see Chapter 3.4.1) and varies between 0.5 and 1 and f_{ct} is defined by Eq. (3.8). The most general way to consider Eq. (4.1) is by inserting the average concrete tensile force ($\sigma_{c,ts} A_{c,ef}$) into the section equilibrium equations (Eqs. (3.58) and (3.59)). For tension chords with constant section properties and tension forces (that is $V = 0$ in bending elements) this yields the average steel strain reduction

$$\Delta \epsilon_{s,ts} = \frac{\lambda f_{ct} (1 - \rho_{ef})}{2 \rho_{ef} E_s} \quad (4.2)$$

and the corresponding average curvature reduction

$$\Delta \chi_{ts} = \frac{\Delta \epsilon_{s,ts}}{d - x_{II}} \quad (4.3)$$

for tension chords in bending elements (Fig. 4.1 (d)). The latter equation assumes a constant compression zone height (x_{II}), which allows its superimposition with the State II curvature. The main disadvantage of Eqs. (4.2) and (4.3) is their dependency on the effective reinforcement ratio of the tension chord $\rho_{ef} = A_s / (A_{c,ef} + A_s)$.

Marti (2004) suggested determining the effective reinforcement ratio by equating the State II steel stresses in the actual bending element and the corresponding steel stresses in the tension chord at cracking. In bending members without axial forces ($N = 0$), the State II steel stresses at $M = M_r$ are equal to $\sigma_{s,II,r} = (M_r n (d - x_{II}) / I_{II})$, while the corresponding steel stresses in the fictitious tension chord are equal to $\sigma_{s,II,r} = f_{ct} (1 / \rho_{ef} + n - 1)$. Solving for ρ_{ef} , leads to

$$\rho_{ef} = \left[\frac{n I_I (d - x_{II})}{I_{II} (h - x_I)} - n + 1 \right]^{-1} \quad (4.4)$$

and a net concrete area

$$A_{c,ef} = n A_s \left[\frac{I_I (d - x_{II})}{I_{II} (h - x_I)} - 1 \right] \quad (4.5)$$

In contrast to Schiessl's effective reinforcement ratio (Eq. (2.8)), Eq. (4.4) is compatible with the Bernoulli bending theory. Inserting Eq. (4.4) into Eq. (4.2) leads to

$$\Delta \epsilon_{s,ts} = \frac{\lambda}{2} \left[\epsilon_{s,II,r} - \frac{f_{ct}}{E_c} \right] \quad (4.6)$$

while Eq. (4.4) in Eq. (4.3) produces

$$\Delta \chi_{ts} = \frac{\lambda}{2} \left[\frac{M_r}{E_c I_{II}} - \frac{f_{ct}}{E_c (d - x_{II})} \right] \quad (4.7)$$

The first terms in the brackets of Eqs. (4.6) and (4.7) correspond to the State II steel strain and curvature, respectively at $M = M_r$. The 2nd term in Eq. (4.6) represents the State I steel strains at $M = M_r$, while the second term in Eq. (4.7) represents those State I steel strains divided by the State II steel lever arm. Both equations are load-independent. The fact that they could have been derived directly from Fig. 4.1 (a) for $M = M_r$ proves the consistency of the approach.

Eqs. (4.1) and (4.6) form the basis for crack width predictions, while Eq. (4.7) is a very practical equation for considering tension stiffening in bending elements, as the effective reinforcement ratio is implicitly considered. Eqs. (4.6) and (4.7) are derived for $V = 0$, but represent good approxi-

mations also when $V \neq 0$, as the tension force gradient due to shear within the cracked elements is usually small (see Seelhofer (2009)).

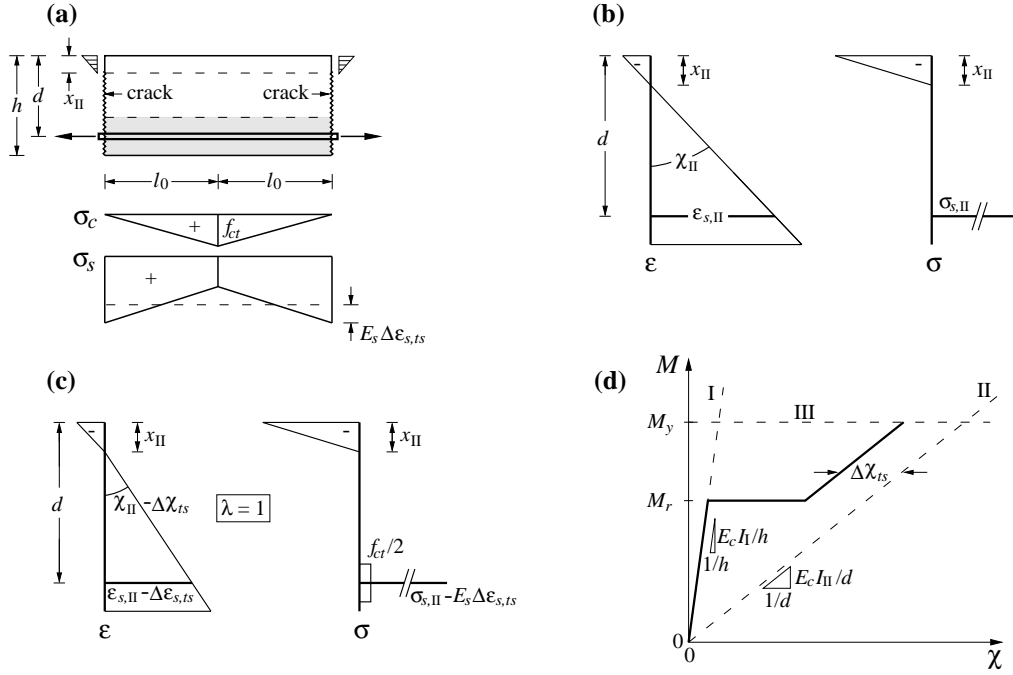


Fig. 4.1 Tension stiffening in a cracked flexural member ($N = 0$): (a) Tension chord element between two cracks; (b) strains and stresses in State II section; (c) average strains and stresses considering tension stiffening ($\lambda = 1$); (d) moment-curvature diagram illustrating $\Delta \chi_{ts}$.

For combined bending and axial force (notation see Fig. 3.5), the procedure described above leads to:

$$A_{c,ef} = A_s \left[\chi_{II,r} (d - c_{II,r}) \frac{E_s}{f_{ct}} - n \right] \quad (4.8)$$

and

$$\rho_{ef} = \left[\chi_{II,r} (d - c_{II,r}) \frac{E_s}{f_{ct}} - n + 1 \right]^{-1} \quad (4.9)$$

as well as

$$\Delta \chi_{ts} = \frac{\lambda}{2} \left[\chi_{II,r} \frac{d - c_{II,r}}{d - c_{II}} - \frac{f_{ct}}{E_c (d - c_{II})} \right] \quad (4.10)$$

Note that Eq. (4.10) is load-dependent. $\chi_{II,r}$ and $c_{II,r}$ denote the State II curvature and height of the compression zone at cracking.

4.1.2 Long-Term

Under sustained loads, creep relaxes the concrete stresses involved in the mechanical interlock between the steel and the concrete (Fig. 4.2 (a)). As a consequence, the effective bond stresses are reduced and the slip is increased. In order to consider the loss of bond stress due to creep, factor

$$k_{\varphi} = \frac{\tau_{b,\varphi}}{\tau_b} = \frac{E_{c,ef}}{E_c} = \frac{1}{1 + \varphi} \quad (4.11)$$

is introduced. This factor (Fig. 4.2 (b)) is determined according to the Effective Modulus Method (Eq. (3.65)) and used to reduce the concrete strains

$$\varepsilon_{c,ts} = k_{\varphi} \frac{\lambda f_{ct}}{2E_c} \quad (4.12)$$

and the steel strain reduction

$$\Delta\varepsilon_{s,ts} = k_{\varphi} \frac{\lambda}{2} \left[\varepsilon_{s,II,r} - \frac{f_{ct}}{E_c} \right] \quad (4.13)$$

The crack spacing of existing cracks is not affected by bond creep and λ remains between 0.5 and 1. Besides bond creep, the average curvature reduction

$$\Delta\chi_{ts} = k_{\varphi} \frac{\lambda}{2} \left[\frac{M_r}{E_c I_{II}} \frac{(d - x_{II})}{(d - x_{II,ef})} - \frac{f_{ct}}{E_c (d - x_{II,ef})} \right] \quad (4.14)$$

is further affected by the drop in the neutral axis due to compression zone creep. The height of the compression zone $x_{II,ef}$ is determined with the effective elastic modulus (Eq. (3.65)).

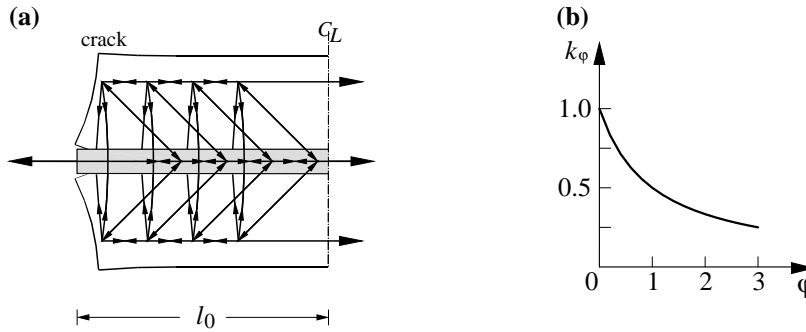


Fig. 4.2 Long-term loss of tension stiffening: (a) Schematic illustration of the internal stress resultants involved in the mechanical interlock between the steel and the concrete in a cracked RC tension chord; (b) loss of bond stress under sustained loads according to Eq. (4.11).

Neglecting the shrinkage restraint between the steel and the cracked concrete, shrinkage further increases the slip without influencing the bond stresses. The assumption of a constant bond stress, which is reduced in time due to bond creep, impedes the modelling of secondary cracks caused by restrained shrinkage stresses in the tensile concrete between the cracks. If at all, secondary cracks are most likely to form in $\lambda = 1$ crack elements and are therefore included within the range of $\lambda = 0.5$ to 1.

The strongly simplified relationship between k_{φ} and φ (Fig. 4.2 (b)) is suggested in view of the highly complex nature of the stresses involved in the mechanical interlock and the large uncertainties involved in determining the long-term concrete parameters. Note that while λ [0.5...1] takes into account the crack spacing, k_{φ} [0...1] considers the contribution of the tensile concrete between the cracks, where $k_{\varphi} = 1$ implies $\tau_b = 2f_{ct}$ and $k_{\varphi} = 0$ implies $\tau_b = 0$. In this sense, k_{φ} can be seen as a general factor for expressing the contribution of tension stiffening for a given crack spacing. k_{φ} is used in